-RESEARCH PAPER-

International Journal of Mining and Geo-Engineering

IJMGE

IJMGE 59-1 (2025) 91-96

DOI: 10.22059/IJMGE.2025.386171.595207

The application of an integral-equation-based automatic inversion algorithm for interpretation of vertical electrical sounding data

Seyed Hossein Hosseini [a], Ramin Varfinezhad [a, *], Saeed Parnow [b, c], Saeed Ghanbarifar [a], Maysam Abedi [d] and Ali Asghar Ghasemi [e]

[a] *Institute of Geophysics, University of Tehran, Tehran, Iran.*

[b] *School of Computing and Engineering, University of West London (UWL), London, UK.*

[c] *The Faringdon Research Centre for Non-Destructive Testing and Remote Sensing, University of West London, London, United Kingdom of Great Britain and Northern Ireland.*

[d] *School of Mining Engineering, Faculty of Engineering, University of Tehran, Iran.*

[e] *Faculty of Sciences, Razi University, Kermanshah, Iran.*

Article History:

Received: 28 November 2024.

Revised: 03 February 2025.

Accepted: 12 February 2025.

ABSTRACT

This study presents the implementation of an automatic inversion algorithm designed for the analysis of direct current (DC) vertical electrical sounding (VES) data, utilizing a one-dimensional (1D) linear integral equation approach. The forward modelling problem was derived from a three-dimensional (3D) integral equation, which was elegantly simplified through numerical integration across horizontal dimensions. The inverse problem was tackled through a minimum length solution that integrated a depth-weighting function and optimized the regularization parameter based on the maximum value of the forward operator. The efficacy of this algorithm was validated by inverting synthetic datasets as well as by its application to real field data. The results highlighted the limitations inherent in 1D inversion, particularly in cases where a layered Earth is significantly violated, as evidenced by comparisons with two-dimensional inversion models. In contrast, in contexts characterized by predominantly layered subsurface structures, the algorithm successfully produced accurate representations of the subsurface models. These findings underscore the method's efficacy in various geological environments, offering a robust tool for geophysical exploration.

Keywords: *DC resistivity, Electrical resistivity sounding, Vertical Electrical Sounding (VES), Integral equations..*

1. Introduction

In recent decades, geophysicists have engaged in a meticulous and systematic effort to gather and analyze diverse geophysical data to examine structural features, natural resources, and the internal composition of the Earth. Comprehensive studies have resulted in the evolution of a diverse suite of quantitative and qualitative methodologies, which serve to decode these complex datasets, thereby revealing the concealed subsurface geometries. Inversion techniques are crucial in this context, facilitating the recovery of subsurface physical properties, such as density variations, magnetization, conductivity, and chargeability, from both ground and aeromagnetic geophysical surveys, which may exhibit either linear or nonlinear relationships with observed anomalies [1-9].

Geophysical modelling and inversion are primarily conducted in three dimensions (3D); however, certain cases may need different methodologies. For instance, when the subsurface target extends infinitely in a horizontal plane, particularly along the y-axis, a two-dimensional inversion is suitable. Conversely, if the subsurface configuration varies only in the vertical direction, one-dimensional (1D) inversion is applicable. The focus of this study is on the 1D direct current (DC) resistivity method, known as vertical electrical sounding (VES), which has been employed in several practical applications (e.g., [10-14]). The inverse problem, while inherently nonlinear, may be reformulated in a linear form given certain assumption. This transformation leverages the 3D linear integral equation framework established by Perez-Flores et al. (2001) for DC resistivity methods [15]. A 1D problem for DC resistivity is derived by applying numerical integration over both horizontal axes from negative to positive infinity. The nonlinear 1D problem yields an exact solution compared to the linear method; however, the latter is frequently favored for various practical reasons. Linear inversion necessitates the computation of the forward operator matrix only once during the iterative inversion process, whereas nonlinear inversion requires recalculating the Jacobian matrix at each iteration. Additionally, the forward operator derived from linear inversion can be reused across all datasets with uniform electrode spacing, a common scenario in practice. Moreover, nonlinear inversion is significantly influenced by the choice of the initial model; an inappropriate selection may result in convergence to a local minimum, resulting in a geologically infeasible solution.

In contrast, the linear approach requires merely an initial homogeneous model with resistivity established at the average of the observed apparent resistivities. Another advantage of the linear method is that it allows for the discretization of the subsurface into numerous

* Corresponding author. *E-mail address:* ramin.varfi@ut.ac.ir (R. Varfinezhad).

thin layers, eliminating the need to estimate the number of layers and facilitating a flexible and reliable inversion process. Finally, this vertical layer-by-layer discretization enables the efficient construction of pseudo-2D inverse sections by aligning multiple 1D inverse models along the same line, a capability also achievable using nonlinear algorithms.

This research presented a 1D linear inversion technique for DC resistivity sounding data, utilizing a regularized weighted minimum length solution. The model weighting function was established by depth weighting, and the regularization parameter was determined based on the maximum value of the forward operator. To establish the efficacy of the forward operator, its results were rigorously compared with those obtained from a nonlinear formulation, enabled a comprehensive assessment of accuracy and computational efficiency. The efficacy of the inversion process was then validated by the inversion of synthetic datasets. Finally, two exemplary cases studied from real-world applications were examined. The first scenario demonstrated the limitations of 1D inverse modelling in accurately representing the subsurface when the assumption of a layered Earth is significantly violated. This limitation was emphasized by comparing 2D inverse models with pseudo-2D sections derived from the 1D inversion results. Conversely, the second case, characterized by a layered geological structure, showcased the efficacy of 1D inversion technique in accurately reconstructing a plausible subsurface model, thereby validated its applicability in such scenarios.

2. Methodology

2.1. Forward modelling

The 3D linear integral for DC resistivity method can be formulated as [15]:

$$\log \rho_a(r_A.r_B.r_M.r_N) = \frac{C}{4\pi^2} \times \int M(r_A.r_B.r_M.r_N.r') \times \log \rho_a(r')\, d^3\, r' \quad (1)$$

where C represents the geometrical factor of the array, given by $\frac{L^2}{2l}$ for the Schlumberger configuration, $2l$ is the distance between the potential electrodes, and $2L$ is the distance between the current electrodes (see Fig. 1). The parameters r_A, r_B, r_M, r_N and r' denote the position vectors of electrodes A, B, M, N and the source, respectively.

The 1D forward problem can then be derived by performing a numerical integration of Eq. (1) along the x and y directions from negative to positive infinity. A similar approach was previously applied to transform the 3D to a 2D problem for the DC resistivity method by Varfinezhad et al. (2022) [16].

The integral form of the corresponding inverse problem can be expressed as a Fredholm Integral Equation of the First Kind (IFK), which can be represented as:

$$d(s) = \int G(sz)m(z)dz \quad (2)$$

where s represents the current and potential electrodes, d denotes the forward response (data), z is the depth of the centers of the assumed layers, G is the forward operator kernel and m denotes the model parameter. The integral Eq. (2) is discretized into a compact algebraic form after a proper discretization:

$$d = Am \quad (3)$$

where d is a column vector containing the observed apparent electrical resistivity data. The vector m contains M unknowns, and A is an N × M discretized forward matrix.

2.2. Inversion algorithm

Concerning the inversion of DC resistivity data, the minimum length solution of Eq. (3) reads (e.g., [17]):

$$\mathbf{m} = \mathbf{m}_0 + (\mathbf{W}_m^{-1}\mathbf{A}^{\mathbf{T}})(\mathbf{A}\mathbf{W}_m^{-1}\mathbf{A}^{\mathbf{T}} + \mu\mathbf{W}_d)^{-1}(\mathbf{d} - \mathbf{A}\mathbf{m}_0) \quad (4)$$

where $\mu > 0$ is the regularization parameter used to manage the possible ill-conditioning of the problem and is selected based on the maximum value of the forward operator. Eq. (4) serves as an approximation of the nonlinear 1D resistivity problem, with the final solution being achieved iteratively:

$$\mathbf{m_k} = \mathbf{m}_{k-1} + (\mathbf{W}_m^{-1}\mathbf{A}^{\mathbf{T}})(\mathbf{A}\mathbf{W}_m^{-1}\mathbf{A}^{\mathbf{T}} + \mu\mathbf{W}_d)^{-1}(\mathbf{d} - \mathbf{A}\mathbf{m}_{k-1}) \quad (5)$$

where k denotes the iteration number. The primary advantage of the linear solution over the nonlinear approach lies in the fact that the matrix $\mathbf{A}$ remains constant throughout the iterations, whereas the nonlinear method requires computing the partial derivatives of simulated data with respect to the model parameter (the Jacobian matrix) at each iteration. The weighting matrix $\mathbf{W}_m$ (as referenced in Eqs. 4 and 5) is often chosen as $\mathbf{W}_m = \mathbf{C}^{\mathbf{T}}\mathbf{C}$, where $\mathbf{C}$ may represent, for example, the steepness matrix or the roughness matrix. Building on the algorithms developed for 2D inversion of DC resistivity data [18-19], we utilized depth weighting of the form:

$$\mathbf{W}_m = \frac{1}{z_c{}^{\beta}} \quad (6)$$

Here, z_c represents the depth coordinates of the cell centers, and β is the depth weighting exponent. A previous study in [16] has demonstrated that $\beta = 1$ is optimal for DC resistivity inversion . In this study, the same value was adopted.

3. Numerical simulation

The numerical simulation unfolded in a meticulously crafted two-phase process. Initially, the precision of the linear forward operator was assessed by comparing its results with those derived from a nonlinear formulation. Subsequently, synthetic data generated from an exact method was utilized for inverse modelling. To ensure a comprehensive evaluation, the performance of the linear approach was tested against data obtained from the exact solution. Furthermore, to delve deeper into the algorithm's resilience, random noise was introduced into the synthetic data, allowed for a comprehensive examination of the stability and robustness of the inversion algorithm employed.

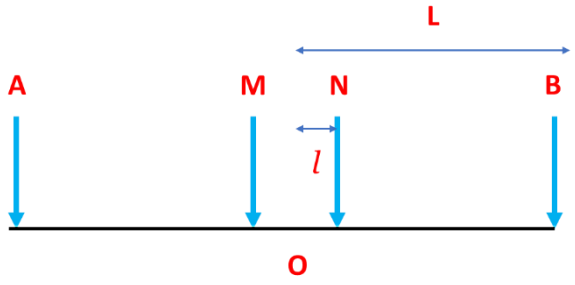

Figure 1. Schematic representation of the Schlumberger array configuration. Points A and B represent the current electrodes, while M and N denote the potential electrodes. The distances 2L and 2l correspond to the separation between the current electrodes and the potential electrodes, respectively, with O representing the midpoint of the array

3.1. Forward operator performance

Prior to conducting the inversion of 1D DC resistivity data, it is essential to evaluate the efficacy of the forward operator. To achieve this, a three-layered model exhibiting a decreasing resistivity trend was utilized (see Fig. 2). The performance of the linear forward operator in 2D modelling of the DC resistivity method has been previously analyzed by Varfinezhad and Oskooi (2020) [19]. This study compared and illustrated the apparent resistivity curves derived from both the one-dimensional nonlinear and linear equations for the specified model in Fig. 2 that are compared and illustrated in Fig. 3. As expected, the curves did not align perfectly, indicated some discrepancies in the results from the linear method compared to those from the nonlinear approach. The qualitative performance of the linear forward operator was promising.

Quantitatively, the root-mean-square (RMS) misfit error for the linear equation, when compared to the nonlinear solution, was measured at 2.23%, indicated the efficiency and reliability of the forward operator.

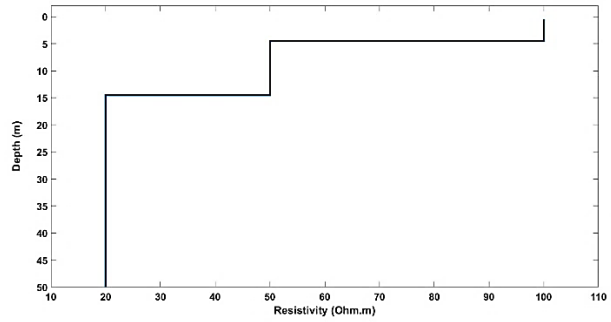

Figure 2. Synthetic model containing the three-layered Earth.

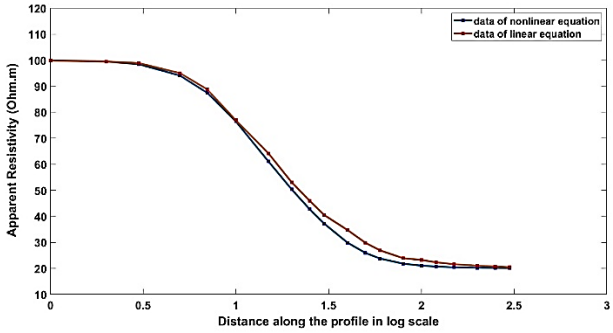

Figure 3. Forward response computed by the linear integral equation versus data calculated from nonlinear equation. RMS error of the linear method was 2.23%.

3.2. Synthetic data inversion

This section assessed the 1D linear inversion algorithm using a three-layered medium. The first layer extended from the surface to a depth of 5 meters, exhibited a resistivity of 50 Ω·m. The second layer ranged from 5 to 15 meters in depth with a resistivity of 100 Ω·m, and the third layer had a resistivity of 20 Ω·m (see Fig. 4). The synthetic data used in this analysis were generated through a nonlinear equation, with an addition of 5% random noise to simulate measurement errors. To ensure an equitable assessment of the proposed linear inversion algorithm, it is crucial that the synthetic data be created using the nonlinear equation. The resulting inverted model is illustrated in Fig. 4.

The inversion method demonstrated a remarkable efficacy in reconstructing the true model, with only slight discrepancies. Specifically, the resistivity of the first layer was underestimated by 3 Ω·m, and there were minor inaccuracies in the estimated thicknesses of the layers. Notably, while the subsurface was divided into 50 layers during the inversion process, the final recovered model simplified to three layers, aligned with the true model. This remarkable flexibility intrinsic to the linear inversion technique offered a distinct advantage, as it was not easily replicated with nonlinear methods.

4. Real data

Inspired by the successful results of the 1D inversion algorithm on synthetic data, we expanded its application to two real-world datasets, which exemplified its practical applicability.

4.1. Real data of Chobin area

The study area is located at longitude 622153 East and latitude 3806089 North within the UTM WGS 1984 coordinate system. It is positioned 1130 meters west of Chobin village in the Gehwarah district of Kermanshah Province, Iran. A visual representation from Google Earth illustrates the survey area, highlighting the positions of the gathered vertical electrical sounding (VES) and profile data, as shown in Fig. 6.

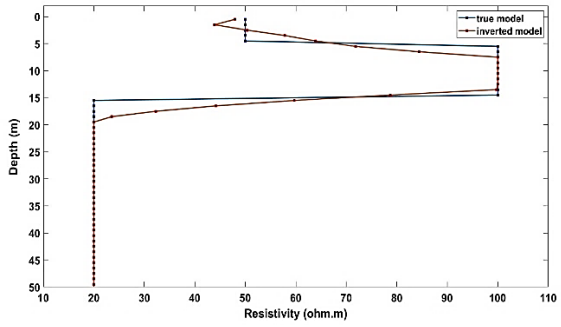

Figure 4. The comparison of the true and inverted model from 5% noisy data.

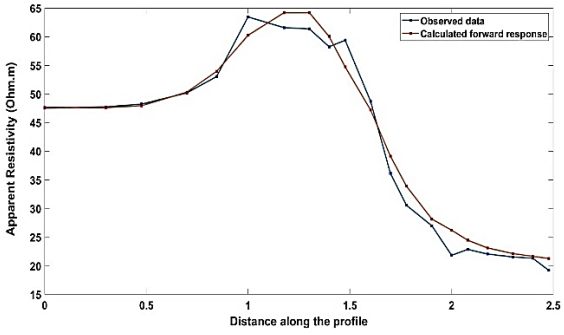

Figure 5. The comparison of the observed and computed data.

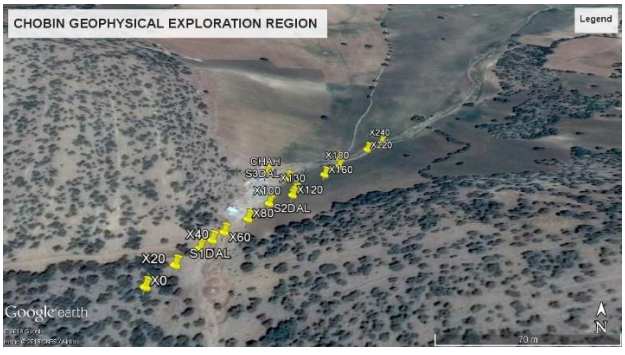

Figure 6. A view of the survey area and locations of the profile and all three soundings (S1DAL, S2DAL, and S3DAL).

The exploration site is situated within the Kashkan formation, characterized by its rich conglomerate, sandstone, and striking red marl. The site is bordered to the north by the Amirs formation and to the south by the Shahbazan formation. The geological units of conglomerate and marl from the Kashkan formation, alongside the dolomite of the Shahbazan formation, display low permeability, resulting in insufficient drainage throughout the area The geological age of these formations ranges from the Paleocene to Eocene epochs.

In the Chobin area, data were gathered through vertical electrical sounding (VES) using the Schlumberger array and Electrical Resistivity Tomography (ERT) with a dipole-dipole configuration. The VES dataset comprised three distinct soundings, including S1DAL, S2DAL, and S3DAL, while the ERT profile runed along the same survey line. This profile extends a total of 240 meters, with the centers of the soundings located at 40 m, 100 m, and 140 m from the beginning of the profile. The inverted models generated from the VES data, along with their corresponding computed forward responses compared to the observed data, are illustrated in Fig. 7.

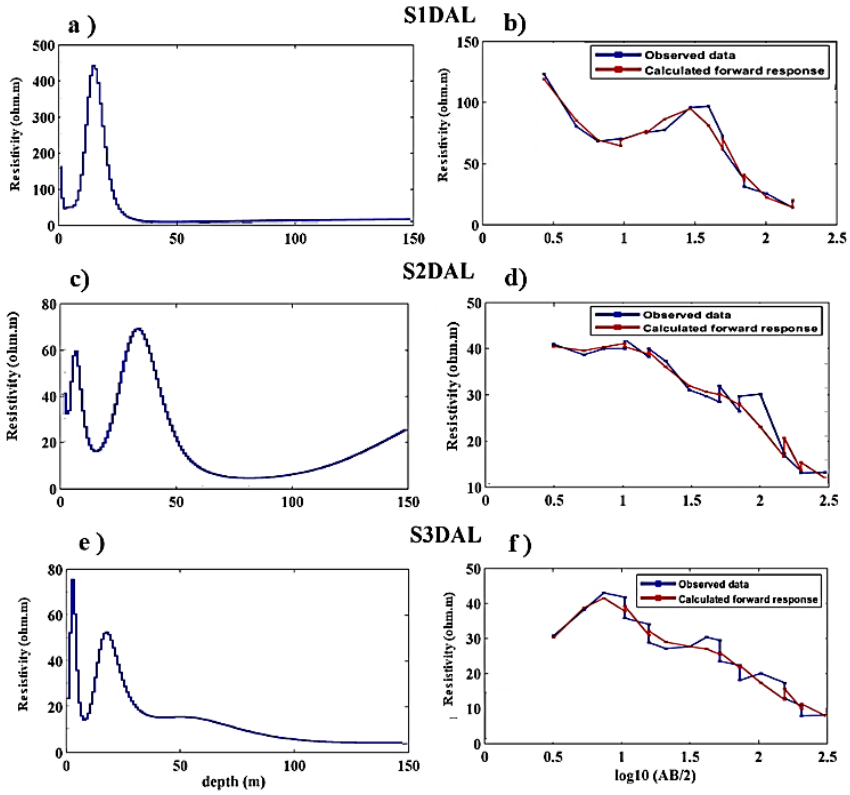

Figure 7. Inverted models (left column) alongside measured data compared to computed data from inverse models (right column) for all soundings, labelled from (a) to (f).

Fig. 7 clearly shows that the inverted resistivity models for the three soundings display distinct variations in resistivity with depth. For S1DAL, there was a sharp decrease in resistivity with depth, indicated a transition from a resistive layer to a conductive one. S2DAL presented a more intricate resistivity profile, featured an intermediate resistive layer and an underlaid conductive zone, which suggested potential lithological or hydrogeological changes. Similarly, S3DAL exhibited a resistive upper layer that transitioned into a less resistive lower layer. The close alignment between the observed data and the calculated forward responses for all three soundings reinforced the reliability of the inversion results.

By arranging these 1D inversion models side by side, a pseudo-two-dimensional inverse section (Fig. 8, top) was created. For comparative analysis, a 2D inversion model derived from the ERT data is shown in Fig. 8 (bottom). A notable discrepancy was observed between the pseudo-2D section and the 2D inversion results. This divergence can be attributed to the limitations of the 1D approach when the subsurface structure significantly deviated from the layered-Earth assumption. In such instances, the 1D inversion model fails to yield a realistic solution, necessitating more advanced 2D or even 3D inversion techniques.

The 2D inversion model identified four prominent faults within the subsurface, provided a more accurate depiction of the geological complexities in the area. In contrast, the pseudo-2D section oversimplified the subsurface structure and did not adequately capture these fault zones. This underscores the need for higher-dimensional inversion methodologies when interpreting regions characterized by substantial structural heterogeneity.

4.2. Real data of Gokceada

For the second real data set, a Schlumberger sounding and an ERT profile were utilized. The data were collected in Kalekoy, located in the northeastern part of Gokceada (Fig. 9). Gokceada, the largest island of Turkey, lies within an active tectonic region with coordinates ranging from [40° 05′ 12″ to 40° 14′ 18″] N and [25° 40′ 06″ to 26° 01′ 05″] E [20]. The surface geology of Gokceada consists of a thick sedimentary sequence, volcanic rocks, and alluvium [21]. The sedimentary sequence, comprising conglomerate, sandstone, shale, siltstone, limestone, and intercalated coal seams, was deposited during the Early Eocene to Late Oligocene period [22].

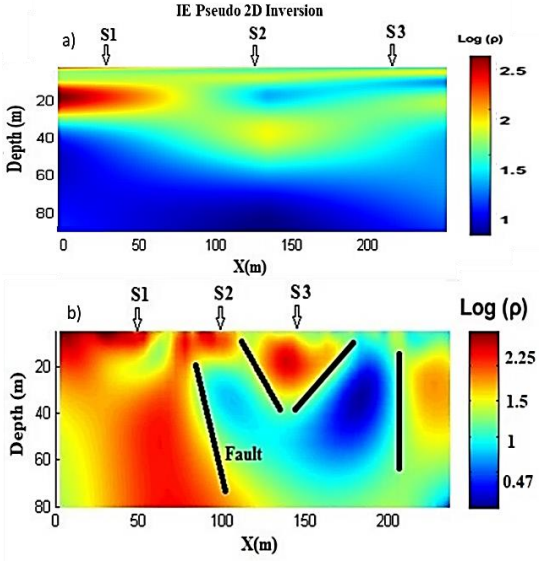

Figure 8. Comparison between the pseudo 2D inverse section and the 2D inverse model, marked with titles (a) and (b). The interpreted potential faults are also highlighted.

The ERT data were collected using a dipole-dipole array with an electrode spacing of a=10m and n values ranging from 1 to 7. The inversion model derived from the ERT data revealed that the subsurface is predominantly horizontally layered with distinct resistivity variations (Fig.10a). Given this horizontal layering, the 1D inversion of the

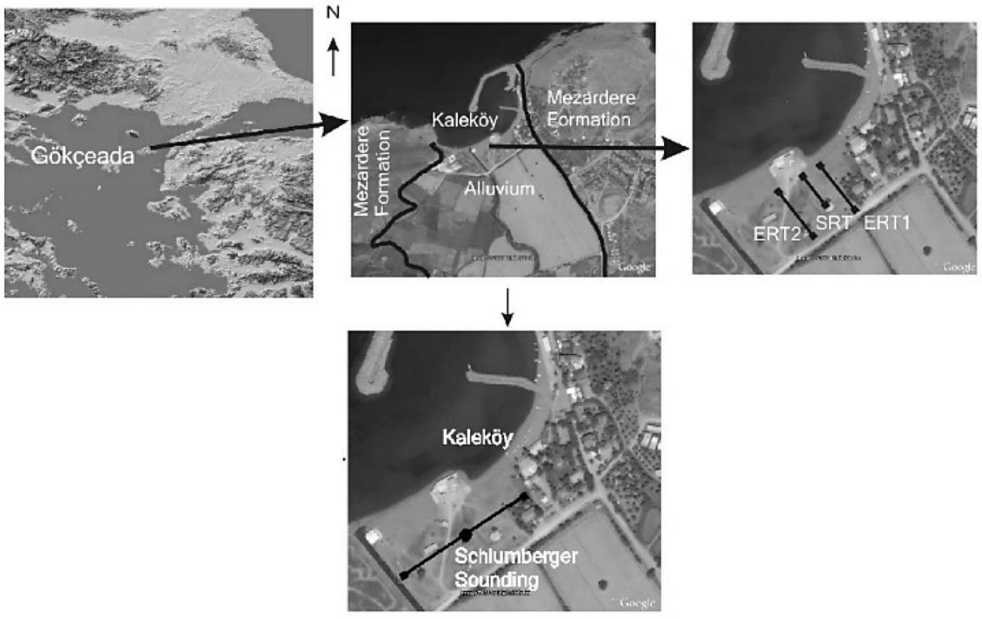

Figure 9. The location map of site and the position of the profiles (from [21-22] which are not scaled).

Schlumberger sounding data was expected to provide a realistic model, especially for depths greater than 27 m. Based on geological information and the 1D inversion model (Fig. 10b), the top layer was identified as consolidated alluvium extending to a depth of approximately 2 m. The second layer represented a water-saturated zone reached a depth of about 11 m. The third layer, the most conductive, extended to a depth of approximately 25 m and was attributed to seawater intrusion. Below the third layer, an increase in resistivity suggested the presence of the Mezardere formation. These interpretations were consistent with the results from the ERT data inversion. In conclusion, the 1D inversion method proved highly effective in subsurface investigations where the geological structure was approximately horizontal.

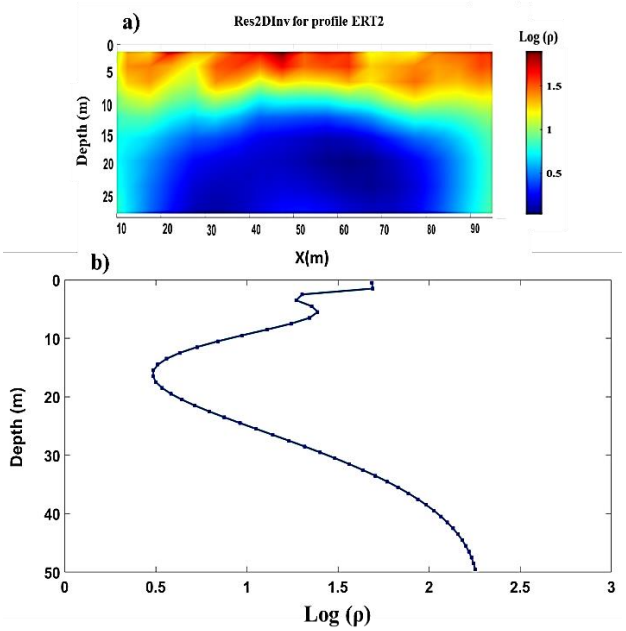

Figure 10. Electrical resistivity imaging in Gokceada region, (a) 2D ERT modelling, and (b) 1D VES modelling.

5. Conclusion

This study presents an effective inversion algorithm for the vertical electrical sounding (VES) data, founded on a regularized weighted minimum length solution. The model weighting function employd depth weighting, with an exponent of 1, indicated the optimal value established for two-dimensional DC resistivity data inversion. The regularization parameter was determined objectively based on the maximum output of the forward operator. The one-dimensional problem was derived from the three-dimensional linear integral equation through numerical integration. The accuracy of the one-dimensional forward modelling using the linear integral equation was rigorously assessed, yielded satisfactory results. The efficacy of the utilized inversion technique was further demonstrated through synthetic data, highlighted its robustness and reliability. Subsequently, the algorithm was applied to two real-world datasets, served as instructive case studies.

In the first case, where the subsurface structure deviated significantly from the layered-Earth assumption, the one-dimensional inversion method was unable to generate a realistic subsurface model. In contrast, the second dataset, which aligned with a largely layered subsurface as validated by two-dimensional inversion outcomes, highlighted the efficacy and relevance of the proposed one-dimensional inversion algorithm. These insights underscored the importance of geological context in the selection of inversion methods and demonstrated the promising capabilities of the developed algorithm for real-world geophysical applications.

Acknowledgments

We would like to sincerely thank Prof. Majdi, the Chief Editor of the IJMGE Journal, for handling of our paper. Additionally, we wish to convey our profound gratitude to the reviewers, Dr. Aghazadeh and Dr. Afshar, whose insightful feedback has significantly enhanced the quality of our work, allowing us to refine and elevate this contribution to a higher standard.

References

[1] Hosseini, S. H., Habibian Dehkordi, B., Abedi, M., & Oskooi, B. (2021). Implications for a geothermal reservoir at Abgarm, Mahallat, Iran: magnetic and magnetotelluric signatures. Natural Resources Research, 30, 259-272.

[2] Talebi, M. A., Hosseini, S. H., Abedi, M., & Moradzadeh, A. (2023). 3D inverse modeling of electrical resistivity and chargeability data through unstructured meshing: a case study for travertine exploration. International Journal of Mining and Geo-Engineering, 57(2), 131-140.

[3] Ghanbarifar, S., Ghiasi, S. M., Hosseini, S. H., Abedi, M., Oskooi, B., & Smirnov, M. Y. (2024). Geoelectrical image of the Sabalan geothermal reservoir from magnetotelluric studies. Journal of Applied Geophysics, 224, 105359.

[4] Ghanbarifar, S., Hosseini, S. H., Ghiasi, S. M., Abedi, M., & Afshar, A. (2024). Joint Euler deconvolution for depth estimation of potential field magnetic and gravity data. International Journal of Mining and Geo-Engineering, 58(2), 121-134.

[5] Ghari, H., Parnow, S., Varfinezhad, R., Milano, M., Fourie, F. D., & Tosti, F. (2024). Cross-Gradient Joint Inversion of DC Resistivity and Gravity Gradient Data: A Multi-Disciplinary Approach for Geoscience, Heritage, and the Built Environment. Remote Sensing, 16(23), 4468.

[6] Ghari, H., Varfinezhad, R., & Parnow, S. (2023). 3D joint interpretation of potential field, geology, and well data to evaluate a salt dome in the Qarah-Aghaje area, Zanjan, NW Iran. Near Surface Geophysics, 3`w (3), 233-246.

[7] Varfinezhad, R., Parnow, S., Florio, G., Fedi, M., & Mohammadi Vizheh, M. (2023). DC resistivity inversion constrained by magnetic method through sequential inversion. Acta Geophysica, 71(1), 247-260.

[8] Najaftomraei, M., Moghadam, S., Varfinezhad, R., Goudarzi, A., & Faghih, A. (2024). Subsurface characterization in southeastern Asaluyeh using DC resistivity and ground penetrating radar. International Journal of Mining and Geo-Engineering, 58(4), 423-429.

[9] Parnow, S., Oskooi, B., & Florio, G. (2021). Improved linear inversion of low induction number electromagnetic data. Geophysical Journal International, 224(3), 1505-1522.[10] Hamzah, U., Samsudin, A. R., & Malim, E. P. (2007). Groundwater investigation in Kuala Selangor using vertical electrical sounding (VES) surveys. Environmental Geology, 51(8), 1349-1359.

[11] Kumar, D., Ahmed, S., Krishnamurthy, N. S., & Dewandel, B. (2007). Reducing ambiguities in vertical electrical sounding interpretations: A geostatistical application. Journal of Applied Geophysics, 62(1), 16-32.

[12] Okoro, E. I., Egboka, B. C. E., & Onwuemesi, A. G. (2010). Evaluation of the aquifer characteristic of Nanka Sands using hydrogeological method in combination with Vertical Electrical Sounding (VES). Journal of Applied Sciences and Environmental Management, 14(2).

[13] Sikandar, P., Bakhsh, A., Arshad, M., & Rana, T. (2010). The use of vertical electrical sounding resistivity method for the location of low salinity groundwater for irrigation in Chaj and Rachna Doabs. Environmental Earth Sciences, 60(5), 1113-1129.

[14] Moghaddam, S., Dezhpasand, S., Kamkar Rohani, A., Parnow, S., & Ebrahimi, M. (2017). Detection and determination of groundwater contamination plume using time-lapse electrical resistivity tomography (ERT) method. Journal of Mining and Environment, 8(1), 103-110.

[15] Pérez-Flores, M., Méndez-Delgado, S., & Gómez-Treviño, E. (2001). Imaging low-frequency and DC electromagnetic fields using a simple linear approximation. Geophysics, 66(5), 1067-1081.

[16] Varfinezhad R., Fedi M., & Milano M. (2022). The role of model weighting functions in the gravity and DC resistivity inversion. IEEE Transactions on Geoscience and Remote Sensing, 60(1), 1-15.

[17] Menke, W. (2012). Geophysical data analysis: discrete inverse theory. Academic Press.

[18] Varfinezhad R., Oskooi B., & Fedi M. (2020). Joint inversion of DC resistivity and magnetic data constrained by cross gradients: compactness and depth weighting. Pure and Applied Geophysics, 177(4325-4343).

[19] Varfinezhad, R., & Oskooi B. (2020). 2D DC resistivity forward modeling based on the integral equation method and a comparison with the RES2DMOD results. Journal of Earth and Space Physics.

[20] Ekinci, Y. L., Demirci, A., & Ertekin, C. (2008). Delineation of the seawater-freshwater interface from the coastal alluvium of Kalekoy-Gokceada, NW Turkey. *Journal of Applied Sciences*, 8, 1977-1981.

[21] Ekinci, Y. L., & Demirci, A. (2008). A damped least-squares inversion program for the interpretation of Schlumberger sounding curves. Journal of Applied Sciences, 8, 4070–4078.

[22] Temel, R.O., & Ciftci, N.B. (2002). Stratigraphy and depositional environments of the tertiary sedimentary units in Gelibolu Peninsula and islands of Gokceada and Bozcaada (Northern Aegean Region, Turkey). TAPG Bulletin, 14(2), 17-40.